INSTITUTE OF PHYSICS PUBLISHING JOURNAL OF MICROMECHANICS AND MICROENGINEERING

J. Micromech. Microeng. **16** (2006) 1967–1974 doi:10.1088/0960-1317/16/10/008

Stamps for nanoimprint lithography fabricated by proton beam writing and nickel electroplating

Kambiz Ansari, Jeroen Anton van Kan, Andrew Anthony Bettiol and Frank Watt

Center for Ion Beam Applications, Physics Department, National University of Singapore, 2 Science Drive 3, 117542, Singapore

E-mail: mahabadik@imre.a-star.edu.sg

Received 16 March 2006, in final form 8 June 2006
Published 21 August 2006
Online at stacks.iop.org/JMM/16/1967

Abstract

In the emerging fields of nanoscience and nanotechnology, the demands for low-cost and high-throughput nanolithographic techniques have increased. Nanoimprint lithography is considered as one of the candidates showing high potential for nanofabrication, and here we report a fabrication process that utilizes high-quality nickel stamps with micron features down to sub-100 nm, made using proton beam writing coupled with nickel sulfamate electroplating. The fabricated stamps have a high aspect ratio, with smooth and vertical sidewalls. Nanoindentation and atomic force microscopy (AFM) measurements of the features on the surface of the stamps indicate a hardness of 5 GPa and a sidewall roughness of 7 nm. The stamps have been used for nanoimprint lithography on polymethylmethacrylate (PMMA) substrates and the imprinted patterns show a high degree of reproducibility.

(Some figures in this article are in colour only in the electronic version)

1. Introduction

Nanoimprint lithography (NIL) (also known as hot embossing lithography (HEL)) is a fabrication process where micro/nanostructures are formed by pressing a stamp/mold against a polymer substrate. The polymer is typically thermoplastic [1] or UV (or thermal) curable [2]. Imprint technology has the advantages that high-density and low-dimensional patterns can be transferred into a wide range of polymeric substrates in a single-step parallel pattern transfer over a large area. This allows the rapid fabrication of structures with high quality, low cost and high throughput without the need for complicated and expensive facilities. The ultimate resolution of the patterns fabricated by NIL is primarily determined by the resolution of the features on the surface of the stamp [3, 4], and so the quality of the stamp is an integral feature of NIL. High-resolution stamps are currently made by e-beam lithography and dry etching, and shallow stamps by e-beam lithography and metal lift-off. Li *et al* [5] have evaluated the relative hardness of stamps made out of various materials including Si, SiO_2, poly-Si, SiC, silicon nitride and sapphire. Commercial stamps from these materials, particularly SiO_2, and poly-Si are now available for research and application [6]. Tanguchi *et al* [4] have presented diamond as a candidate mold for nanoimprinting and Pfeiffer and Schulz *et al* [7, 8] have investigated thermosetting polymeric stamps for nanoimprinting. Nickel stamps were fabricated by e-beam lithography and electroplating [9, 10], which exhibit high-resolution features, increased durability, elasticity and hardness, and have been used for industrial applications. Here we present a new process to fabricate high-quality three-dimensional (3D) micro and nanostamps which combines the high potential of a new direct write technique called proton beam writing (PBW) and nickel electroplating. The stamps are of high quality and exhibit smooth, straight and vertical sidewalls with features

down to and below 100 nm, coupled with a high degree of flatness for a high-resolution high-quality 3D pattern transfer.

2. Proton beam writing

Proton beam writing is a high-potential new direct write technique capable of patterning 3D high aspect ratio nanostructures with a high resolution of 20 nm (potentially less), a smoothness of less than 3 nm and aspect ratios of more than 100 [11, 12]. The technique is the proton beam analog to direct electron beam lithography. However, the MeV protons as opposed to electrons can penetrate deep into the resist along a straight path with minimal scattering. The dominant energy transfer mechanism of the proton in matter is to atomic electrons, where short-range secondary electrons are produced very close to the path of the incident beam. The secondary electrons lead to chain scission in the case of positive resist (e.g. PMMA) or cross linking in the case of negative resist (e.g. SU-8). The small angle scattering and spatial confinement of the deposited energy involved results in high aspect ratio high-resolution 3D structures with vertical sidewalls and sharp edges. In addition PBW has the capability of fabricating dense structures, since there are minimal proximity effects due to the short range of the secondary electrons. Due to the rigidity (high momentum) of the proton beam there are also less problems with surface charging, and although currently PBW does not have the sub-10 nm resolution capabilities of e-beam writing, the focused proton beam exhibits the advantage of an extended depth of focus.

PBW has the potential for fabricating photonic structures [13] by changing the refraction index of the polymer. It also has the capability of modifying surface chemistry through atomic displacement, and this aspect has been used in combination with electrochemical etching to pattern 3D structures in silicon and to produce areas with light emitting characteristics on the surface of silicon [14]. The unique characteristics of PBW can also be used to integrate optical and optoelectronic components into microfluidic structures and this technology offers great potential for fabricating integrated lab-on-a-chip devices. However, as yet an automated user-friendly proton beam writer is not commercially available, although a prototype system has been constructed in the Centre for Ion Beam Applications (CIBA), National University of Singapore [15].

3. Ni microstamp fabrication

In this section, we present the fabrication processes of Ni stamps with micron-size features on its surface. A schematic representation of the process of stamp fabrication using proton beam writing is shown in figure 1. This process involves: (a) coating a conductive seed layer for electroplating onto an Si substrate followed by a spin-coated layer of resist, e.g., PMMA; (b) exposure using proton beam writing; (c) development of the structures; (d) deposition of a second metallization layer on the top surface which acts as a seed layer for the base of the stamp; (e) electroplating of the structures, plus overplating to form the base for the stamp; (e) delamination of the stamp from the substrate and (f) cleaning.

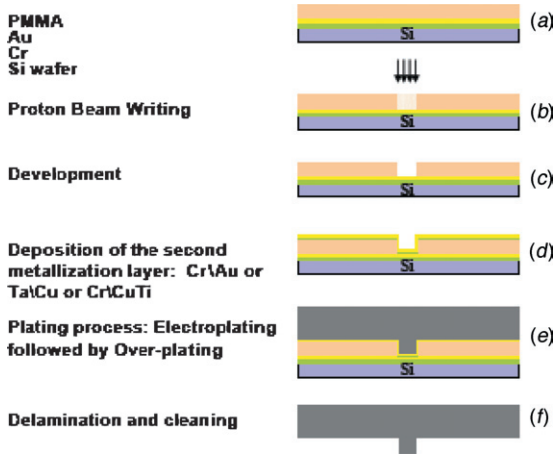

Figure 1. Schematic representation of the process of stamp fabrication using proton beam writing.

3.1. Ni sulfamate electroplating

The Ni electroplating was performed using a commercial plating system from Technotrans AG, RD.50 with a Ni sulfamate bath solution without organic additives at pH 3.5, and 50 °C temperature. The plating substrate was 2 inch wafers, which was coated by a layer of chromium or titanium for adhesion and gold or copper for plating the seed layer (although using copper as a seed layer has the disadvantage that it will oxidize very fast). The coating of the layers was carried out consecutively in a clean room environment using sputtering or e-beam evaporation.

After patterning and developing steps (b) and (c), the step (d) was performed by depositing a layer of Au/Cr on the top of the resist. A two-step electroplating process was then employed: first, electroplating with a very small plating rate up to a height to cover the wafer features (typically 20 μm). This improves the electrolyte transport into the structures with different cross sections and leads to a uniformity of the height of the plated structures over large area. Then the plating current was ramped up to higher values for overplating. However, electroplating at too high, a high plating rate produces stress and intolerable camber at the perimeters which reduces the flatness of the stamp.

A good electric contact is very important to achieve a uniform electroplated stamp. The first plating base deposited at step (a) of our process is required for small patterns only which will be discussed in section 4; however, it also provides a good electric contact for electron transfer from the power supply to the metal ions in the electrolyte. This is to ensure that the structures with micron-size cross sections are filled at similar rate as those with nanosize cross sections over large areas of the wafer that improves the stamp flatness.

Pulse plating has been reported to improve the properties of nickel deposits such as grain size, smoothness and internal stress [16]. To improve the stamp flatness a combination of a pulse-reverse plating process and plating of the sample over a large cathode area to provide a uniform electric field distribution, was employed. Figure 2 illustrates a typical pulse plating process which was used for electroplating of the stamps.

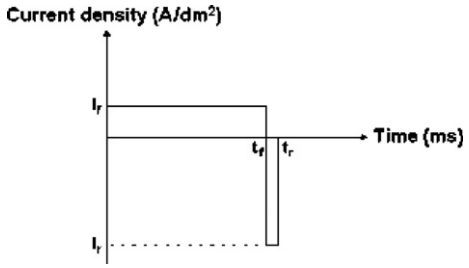

Figure 2. Typical PR waveform with a long small forward current I_f and a short large reverse current I_t which was used for plating of the stamps.

In general, all the electroplating processes were carried out employing first a low current density of 0.4 A dm^{-2}, which leads to a growth rate of 100 nm min^{-1} for the first 20 μm and a high current density of 4 A dm^{-2}, equivalent to a growth rate of 1 μm min^{-1} for the base of the stamp which is typically between 300 and 500 μm thick.

3.2. Microstamp fabrication using PMMA positive resist

We have carried out experiments in both PMMA and SU-8 resists using proton beam writing. Microstamps typically have feature depths from 1 to 30 μm and so we need to achieve relatively thick uniform layers of PMMA resist, which are in general difficult to achieve using a single spin-coat step. A further problem is that PMMA typically has poor adhesion to the plating substrate, and the resist peels off easily during development or electroplating. We have solved these problems as follows: the first step is to sputter on a silicon wafer, a thin layer of Cr or Ti as an adhesion promoter followed by Cu as a plating seed layer. Since copper oxidizes very fast, the wafer was kept in a dry atmosphere prior to PMMA spin coating. A thin layer of 2 μm PMMA resist was spin coated on copper followed by postbaking at 180 °C. During the baking process the copper seed layer changes to black oxide which seems to improve adhesion [17]. To achieve greater PMMA thicknesses multiple consecutive spin–bake processes were then carried out, where the sample was baked at 180 °C for 60 min after every step.

Figure 3 shows SEM images of p-beam-written PMMA structures patterned on a 10 μm thick spin-coated PMMA layer over 3 and 4 inch size wafers using a multilayer spin-coating process where at every step a layer of 1–2 μm resist is spin coated and baked at 180 °C for 2 min. The layer shows a uniformity of 1 μm from center to the edge of the wafer estimated by optical microscope. The sidewalls show uniform layer continuity with no interface marks visible between the consecutively spin-coated layers. Figure 4 shows a SEM image of part of a microstamp fabricated using the plating process as described above, from a p-beam-written PMMA template. The stamp is fabricated in nickel and has parallel ridges with dimensions of 50 μm (width) × 10 μm (height) × 2 cm (length) over a 2 inch size stamp. The stamp exhibits straight smooth vertical sidewalls with sharp edges similar to the mold patterns. The stamps can be cleaned of residual PMMA by soaking in toluene at 40 °C from 1 min (for 2 μm thick PMMA resist) to 1 h (for 50 μm thick PMMA resist).

3.3. Microstamp fabrication using SU-8 negative resist

To fabricate metallic stamps using SU-8 as a mold, we directly spin coated a layer of 20 μm SU-8 10 on Au (200 nm)/Cr (20 nm)/Si, and as with the PMMA process, this exhibited good adhesion. A ridge was patterned in SU-8 using p-beam writing, and after exposure the patterns were developed using the commercially available SU-8 developer. After development, a second metallization layer was deposited on the top of the resist followed by electroplating as described above. To delaminate the stamp from the substrate, they were heated up as they were in contact to 110 °C and immediately were placed between a double-armed vacuum chuck system exerting opposing forces against stretched spring which clamps the sample from the top and bottom. If the process is carried on at high temperature over than glass transition temperature of the polymer, the exerted vertically spring forces pull the stamp–substrate apart and separate them easily. This method is very effective, and reproducible without

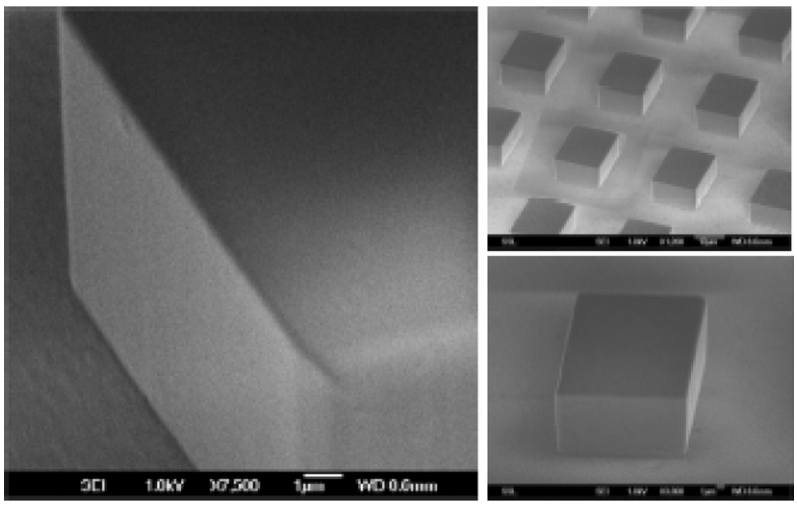

Figure 3. P-beam-written structures in a 10 μm PMMA on a Cu (150 nm)/Ta (20 nm)/Si substrate.

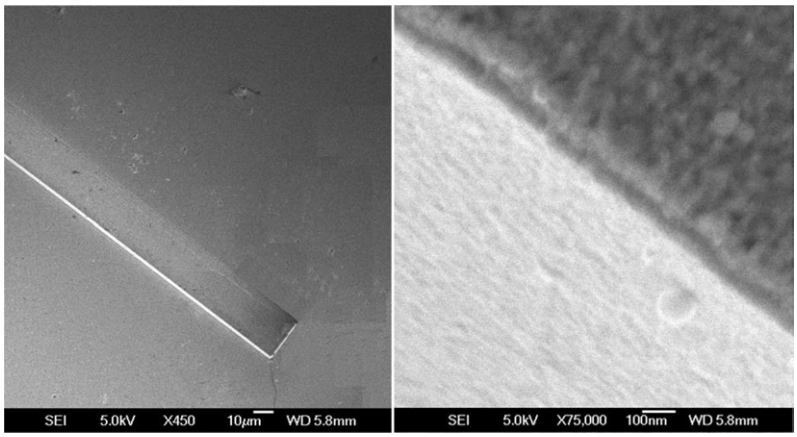

Figure 4. SEM micrographs of a stamp with a Ni ridge of 10 μm (height) $\times$ 20 μm (width) $\times$ 2 cm (length) dimensions, obtained using p-beam-written PMMA as a mold.

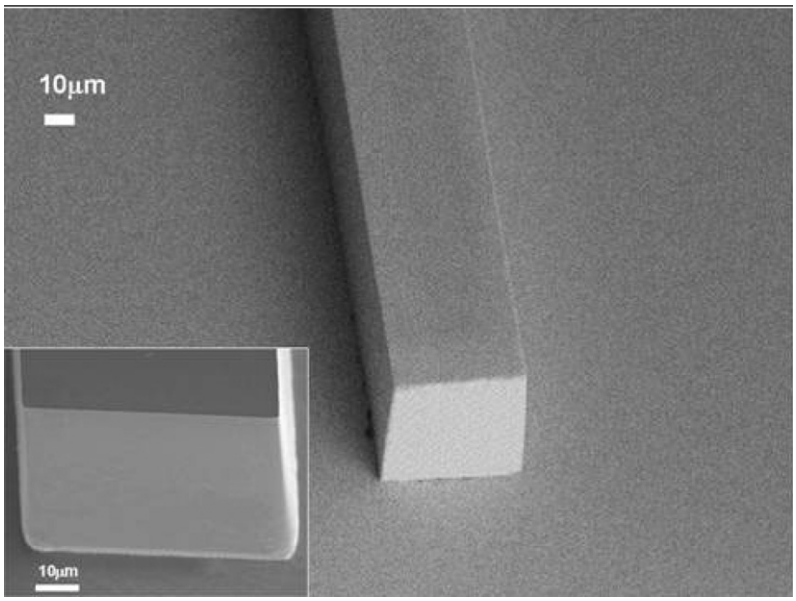

Figure 5. SEM image of a Ni stamp fabricated by p-beam writing using SU-8 as a mold. The stamp consists of ridges with dimensions of 50 μm width, 20 μm depth and 2 cm length supported on Ni base areas.

any damage to the stamp. Figure 5 shows a SEM image of part of a stamp with features consisting of 2 cm long plated ridges.

To clean the stamps of residual SU8, we used chemical etching and ultrasonic agitation at 80 °C to strip off the highly cross-linked exposed SU-8 resist. The chemicals used were SU-8 remover PG from MicroChem Corp. (MCC) plus a short-time cleaning in piranha etches. In extreme cases we additionally placed the sample on hot plate at 300 °C for several hours to burn off the residual resist. Also, the layer of Au/Cr acts as a separator.

It is worth mentioning that PBW of SU-8 negative tone resist (MicroChem Corp (MCC)) has shown consistently excellent resolution comparable to that of PMMA. However, it is still not clear what the ultimate resolution of proton beam writing in PMMA or SU-8 is, and which resist will ultimately demonstrate the highest resolution. Figures 6(*a*) and (*b*) show the high aspect ratio, high resolution structures fabricated by PBW. In this exposure, for PMMA a beam of 2 MeV protons with a beam spot of 200 $\times$ 200 nm^2 and for SU-8 a beam of 2 MeV H_2^+ (equivalent to 1 MeV protons) with a beam spot of 60 $\times$ 120 nm^2 [11] have been used.

Also, with the introduction of new types of resists, more research needs to be carried out to identify the ultimate resolution of p-beam writing [11]. The major drawback of SU-8 however is that the highly cross-linked epoxy produced after exposure is not easy to remove, making it difficult to use as an electroplating mold. Both stamps fabricated by PMMA mold and SU-8 mold show similar smoothness.

4. Ni nanostamp fabrication

Fabricating high aspect ratio 3D nanostamps have added difficulties of void formation in the plated structures, which is particularly common in high aspect ratio structures. Figure 7(*a*) shows SEM images of typical voids in the relief structures on the stamp. Subsequent investigations revealed that during the second metallization process (see figure 1), slight deposition of the metal ions on the sidewalls of the

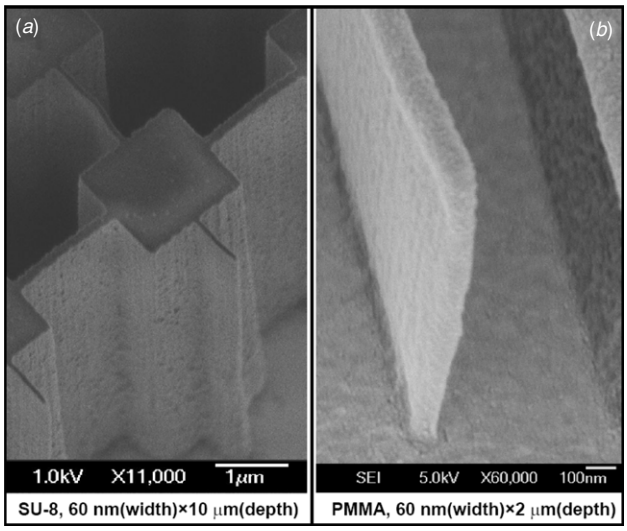

Figure 6. SEM images of 60 nm side walls in SU-8 and PMMA. Both resists show high resolution smooth side walls with high contrast, sharp edges, no undercut, and vertical walls.

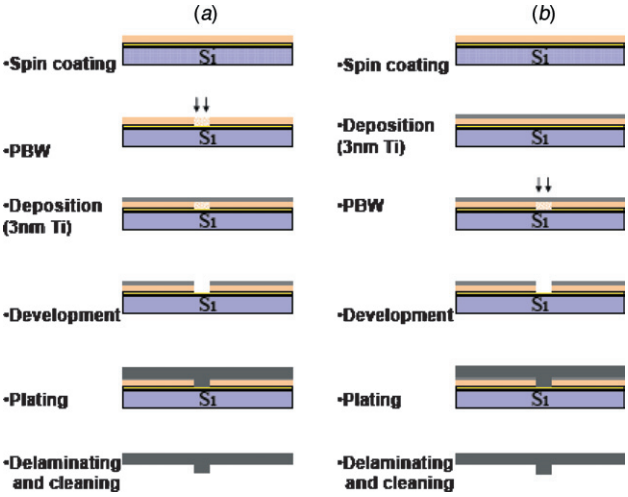

Figure 7. Schematic of the developed nanostamp fabrication processes: (*a*) shows the second method which deposits the second metallization layer first and then develops the patterns; (*b*) shows the first method which involves proton beam writing through the second metallization layer.

developed structures resulted in electric contact between the top metallic layer and the bottom seed layer. Subsequent plating growth on the sidewalls of the trench closes the top of the trench before the bottom plating growth front reaches the top, typically forming voids in the high aspect ratio structures. This appeared to be a problem in nanofeatures for aspect ratios of 5 or more.

Two new approaches were devised to avoid void formation. Both processes rely on plating base-free sidewalls to separate pattern filling from the base layer growth: (1) the deposition of the second metallization layer prior to proton beam patterning; this relies on the proton beam penetrating the second metallization layer and exposing the underlying resist without adverse effects and (2) the deposition of the second metallization layer after proton exposure, but before developing the exposed areas. Both methods rely on the

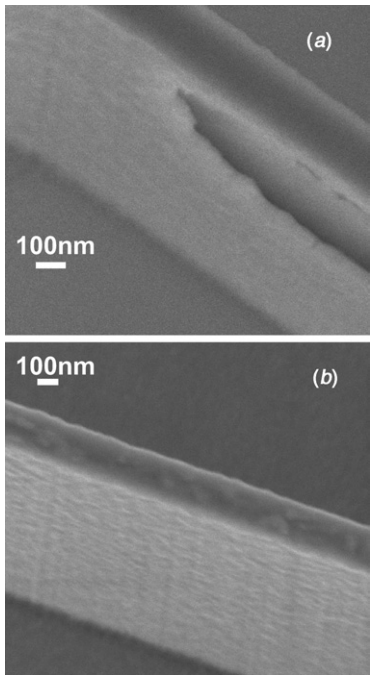

Figure 8. A 200 nm smooth (RMS ∼ 7 nm) high aspect ratio (∼10) stamp: (*a*) with void and (*b*) void free.

penetration of the developer through the second metallization layer, and therefore the second metallization layer should be thin enough so that the structures can be developed but thick enough to provide a conductive layer for the subsequent overplating process. Our experiments indicated that the deposition of a second metallization layer of 3 nm Ti fulfils the above conditions. Figure 8(*a*) shows a SEM image of the typical voids appearing in the 100 nm plated ridges on the overplated nickel base in a continually single-step electroplating process. Figure 8(*b*) shows an example of a void-free ridge stamp using either of the two processes explained earlier and is presented schematically in figures 7(*a*) and (*b*).

5. Next generation stamps (metal-on-metal plating)

The final high-quality master stamp is considered as the most strategically critical requirement for stamp/imprint technology. In order to protect the original high-quality master, a process of metal-on-metal plating (the so-called father–mother–son replication) has been employed, where the initial master is plated to create an intermediate negative metal structure called a mother, which is then used to create a final metal master called a stamper (son). The stamper, an exact replication of the original master, is the end product which can then be used for imprinting. For replication of low aspect ratio metallic structures we use a process borrowed from the CD industry consisting of chemical surface passivation and metal-on-metal plating. In the first stage of production, the metallic structure was immersed in a diluted H_2O_2 solution with 35% concentration for 1 min, and rinsed with deionized water. After chemical treatment, the stamp was plated using the same parameters as for the microstamp fabrication. The typical stamp has dimensions from 2 × 2 cm^2 up to 2 inch

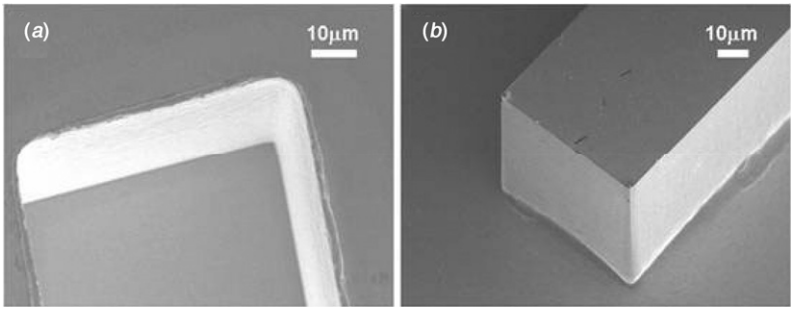

Figure 9. (*a*) SEM image of the Ni mother stamp fabricated from a P-beam-written SU-8 ridge structure (father). (*b*) SEM image of the replicated stamper (son).

size and a base thickness of 300–500 μm. The nickel stamper plated on the nickel stamp substrate was then mechanically delaminated without any pattern distortion. This process has been used for stamps with complex structures such as cross channels and obstacles having low aspect ratios of less than 3, and limited number of patterns. More tests are required for stamps with large number of structures.

Figure 9(*a*) shows a SEM image of the Ni mother stamp fabricated from an SU-8 master written by proton beam writing, and figure 9(*b*) shows the replicated Ni stamper. The SEM images show high-quality replication with smooth straight vertical sidewalls and sharp edges.

6. Stamp characteristics

6.1. Hardness of the stamps

Nanoindentation measurements were carried out to characterize the hardness of the stamps. Due to the small dimensions of the ridges, nanoindentation measurements were performed away from the stamp ridges over an adjacent Ni-plated area of 100 × 100 μm^2, using a UMIS-2000H nanoindenter with a Berkovich indenter tip [18]. Hardness and Young's modulus of 5 GPa and 213 GPa were obtained respectively which is consistent with the previously reported values [19–21] for nickel sulfamate-plated structures. Stamp hardness, which can be optimized, depends on different factors such as bath composition, current density, temperature and the plating process [22]. Experiments were carried out to investigate the influence of the plating current density on the hardness of the stamps using nickel sulfamate bath. Figure 10 illustrates that plating at a low current density (10 mA cm^{-2}) leads to a higher hardness value measured, 5 GPa, whereas by increasing the current density, the hardness falls rapidly and then stabilizes at a value of 3.3 GPa.

For comparison, table 1 presents the hardness of the stamps plated by the nickel sulfamate bath solution, nickel Watts bath solution and the metal-on-metal plated stamper. Every measurement was an average of five tests.

6.2. Sidewall smoothness (RMS) of the stamps

A high-quality stamp exhibits smooth, straight sidewalls with sharp edges and precise geometry, ideal characteristics for imprint applications. High-quality imprint lithography is strongly dependent on the frictional forces at the interface

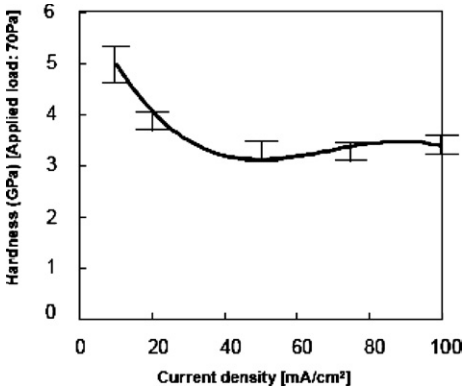

Figure 10. Hardness of the electroplated nickel deposited from nickel sulfamate bath solution versus current density.

Table 1. Hardness and Young's modulus measurements of the plated stamps plated with nickel Watts bath and nickel sulfamate bath. The literature values are from [18, 19].

Materials	Elastic modulus (GPa)	Hardness (GPa)
Nickel (sulfamate bath)	213 ± 5	5.0 ± 0.4
Nickel (Watts bath)	242 ± 2	6.1 ± 0.7
Metal-on metal plated (sulfamate bath)	209 ± 6	5.1 ± 0.3
Literature	207 ± 2	2.7 ± 0.1

of the stamp and the polymer microstructures, which in turn is dependent on the sidewall roughness and the sidewall angles of the stamp features. Calculations and previous measurements indicate a sidewall angle of better than 89.3° for proton beam writing [23].

The smoothness of different surfaces of the fabricated stamps was measured using atomic force microscopy (AFM). The top surface of the plated structures (in contact with the gold seed layer) indicates an RMS roughness of 2.3 nm, whereas the base surface replicates the smoothness of the second metallization layer on the top of the resist and has an RMS roughness of 0.8 nm. Since the grain size of the Ni sulfamate solution is usually more than 1 μm, the electroplated structures appear to replicate the smoothness of the underlying surface.

In order to measure the sidewall roughness of the plated structures, a 50 × 50 μm^2 area of 20 μm thick negative SU-8 resist spun on Au (200 nm)/Cr (20 nm)/Si was irradiated

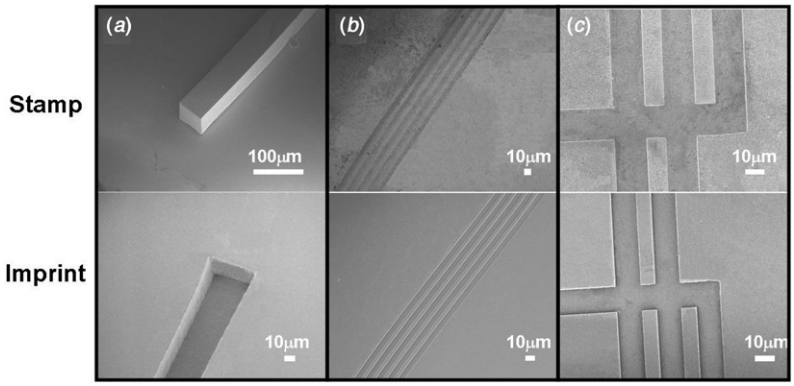

Figure 11. SEM images of nickel stamps used to test the imprinting process. (*a*) SEM image of a stamp consisting of a ridge of 50 μm (width) × 10 μm (height) × 2 cm (length) and its imprinted microchannel. (*b*) A stamp with parallel ridges of 50 μm (width) × 2 μm (height) × 2 cm (length) and its imprinted microfluidic channels. (*c*) A stamp with parallel ridges of 50 μm (width) × 2 μm (height) used to imprint a microchannel intersection.

by a 2 MeV proton beam. After developing the unexposed areas, the structure was plated using the conditions described previously, and the remainder of SU-8 was removed. The structure was fabricated over the edge of the wafer so that after removing the exposed SU-8, the plated sidewall is accessible from the side of the sample. A surface roughness of RMS ∼ 7 nm was measured over an area of 2 × 2 μm^2 by AFM using a Nanoscope III (Digital Instruments) equipped with a silicon tip and operating in the tapping mode.

7. Applications of nickel stamps for nanoimprint lithography

Here we describe tests of our fabricated nickel stamps for nanoimprint lithography. The patterns on the stamps were either elevated features over a large recessed surface (positive relief patterning) or recessed features within a large elevated surface level (negative relief patterning). Stamps with a small dimension of 2 × 2 cm^2 and a big dimension of 2 inch wafer were used for the NIL process. The results presented here are for stamps with positive structures such as parallel ridges, network of ridges with intersections and 90° turning points. The microstamps have micron-size features of 5–50 μm width, 10–30 μm height and up to 2.5 cm length. The nanostamps consisted of features from micron size down to 90 nm width, and 2 μm height. All the patterns were confined in the central regions of the stamps with not more than 2.5 cm^2 areas and low density of typically micron-size displacement. The results presented here are all obtained from two types of PMMA: a 1 mm thick sheet of high molecular weight PMMA (3 × 10^6 g mol^{-1}) and 9.5 × 10^5 g mol^{-1} PMMA spin coated on the silicon wafer.

Nanoimprints were performed in a laboratory-type manual hydraulic press system capable of imprinting 4 inch diameter samples, at 250 °C temperature and 70 bar pressure. Typically, the NIL process of microstamps is accomplished at pressure ranges of 30–40 bars applied at temperature ranges of 140–170 °C with holding times of 20 s up to 1 min, followed by stamp/substrate separation at 110 °C. NIL utilizing nanostamps consisted of high aspect ratio nanostructures require higher pressure values of 40–50 bars, temperature values of 170–190 °C hold for 1–20 min depending on the type of the patterns (positive patterns require shorter time compared to negative patterns) followed by delamination at 110 °C. The PMMA thickness was maintained above the height of the stamp features to prevent damage to the stamp structures.

7.1. Imprinting of microchannels

Figure 11 shows SEM images of a stamp and its imprinted results in a PMMA sheet. The imprint was carried out by heating up the stamp and the PMMA to 170 °C, followed by applying a pressure of 40 bar which was maintained for 20 s, and then releasing the pressure after cooling down to 110 °C.

The replicated structures indicate sharp, vertical and smooth edges similar to the stamp features. After every imprinting, the stamp was cleaned with toluene at 40 °C for 5 min followed by a rinse in deionized water. The stamps have been used for more than 15 times but still more tests are required to clarify the real lifetime of the stamps. The imprinting in thick PMMA sheet leads to polymer bending which can be minimized by using a thin polymer sheet and applying lower temperature and pressure. However, for nanostructures it is essential to apply pressures as high as 40–50 bars at more than 190 °C to achieve a complete pattern transfer over large area.

7.2. Imprinting of high aspect ratio nanochannels

NIL utilizing high aspect ratio nanostamps fabricated by PBW introduces new difficulties. For example, any inaccuracy in the surface parallelism and orientation of the imprint template and substrate can produce side forces which lead to breakage of the stamp features and/or pattern distortion. Our imprints were performed in a hydraulic hard press with flat top and bottom stainless steel chucks, where the pressure is applied vertically to both sides of the imprint stack, the stamp and the substrate. A co-parallelism between the stamp and the substrate minimizes any side forces and provides a uniform pressure distribution with perfect contact over large area and avoids built-up air bubbles at the stamp–substrate interface [24]. The co-parallelism was achieved by using a clamp

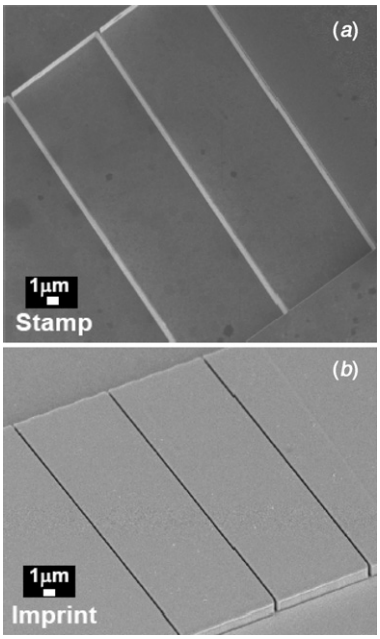

Figure 12. (*a*) SEM image of a Ni stamp consisting of parallel ridges of 100 nm width, 2 μm height connected to 50 × 50 μm^2 platforms and 300 μm thickness of the base areas. (*b*) The results of the imprinting of the stamp in part (*a*) in an 8 μm thick PMMA spin coated on a silicon substrate, showing parallel grooves of nearly 100 nm width, 2 μm height connected to 50 × 50 μm^2 reservoirs showing reproducible fine features, smooth sidewalls and vertical structures.

consisting of top and bottom flat plates which sandwiches the stamp imprint in between and has Euler angles' rotational freedom. This leaves the co-parallelism to the quality of the stamp and plates and their flatness rather than how vertical the external force is needed to be applied. To optimize the stamp flatness we used combinations of reverse-pulse electroplating, EDM wire cutting (electrical discharge machining) and backside polishing plus grinding.

Figure 12 shows an imprint of a high aspect ratio Ni stamp in an 8 μm thick PMMA spin coated on a silicon substrate. The stamps have different dimensions of 2 × 2 cm^2 or 2 inch size and consisted of nanofeatures defined within a total area of 2 mm^2 in the central areas on 300–500 μm^2 base. Our observations indicate that if during the cooling down process we lower the pressures stepwise i.e. decrease the pressure in programmed steps down to zero, then any small lateral movements between the stamp and the substrate can be minimized. Upon separation of the stamp from the substrate no damage either to the stamp or imprinted polymer structures was observed and complete pattern transfer was observed. Since the decrease in stepwise pressure increases the cooling down cycle to much longer time interval, it is still not clear which parameter has more influence on the optimization of the process, and further investigations are necessary to fully understand the process of stepwise releasing.

8. Conclusions

High-quality 3D Ni stamps and molds featuring high aspect ratios as well as smooth vertical sidewalls and sharp straight edges were fabricated by PBW and nickel sulfamate electroplating. The stamp quality was improved by optimizing the plating process and utilizing pulse-reverse electroplating and backside polishing. To protect the original master, a process of metal-on-metal plating was employed (the so-called father–mother–son replication) to copy the master to secondary stampers for imprinting applications. The stamps have been used for nanoimprint lithography and high-quality structures with micron dimensions down to nanosizes were imprinted into PMMA substrates. The imprinted patterns indicate high aspect ratio smooth vertical sidewalls with sharp and straight edges.

References

[1] Chou S Y, Krauss P R and Renstrom P J 1995 *Appl. Phys. Lett.* **67** 3114
[2] Haisma J, Verheijen M, van der Heuvel K and van der Berg J 1996 *J. Vac. Sci. Technol.* B **14** 4124
[3] Kim E, Xia Y and Whitesides G M 1995 *Nature* **376** 581
[4] Taniguchi J, Tokano Y, Miyamoto I, Komuro M and Hiroshima H 2002 *Nanotechnology* **13** 592
[5] Li M T 2003 *PhD Thesis* Princeton University, Princeton
[6] Maximov I, Sarwe E-L, Beck M, Deppert K, Graczyk M, Magnusson M H and Montelius L 2002 *Microelectron. Eng.* **449** 4367
[7] Pfeiffer K *et al* 2002 *Microelectron. Eng.* **61–62** 393
[8] Schulz H, Lyebyedyev D, Scheer H-C, Pfeiffer K, Bleidiessel G, Grutzner G and Ahopelto J 2000 *J. Vac. Sci. Technol.* B **18** 3582
[9] Heidari B, Maximov I and Montelius L 1999 *J. Vac. Sci. Technol.* B **17** 2961
[10] Hirai Y, Kikuta H, Harada S and Tanaka Y 2002 *J. Vac. Sci. Technol.* B **20** 2867
[11] van Kan J A, Bettiol A A and Watt F 2006 *Nano Lett.* **6** 579
[12] van Kan J A, Bettiol A A and Watt F 2003 *Appl. Phys. Lett.* **83** 1629–31
[13] Bettiol A A, Sum T C, Cheong F C, Sow C H, Rao S V, van Kan J A, Teo E J, Ansari K and Watt F 2005 *Nucl. Instrum. Methods* B **231** 364–71
[14] Breese M B H, Teo E J, Mangaiyarkarasi D, Champeaux F, Bettiol A A and Blackwood D 2005 *Nucl. Instrum. Methods* B **231** 357–63
[15] van Kan J A, Bettiol A A, Ansari K, Shao P and Watt F 2004 *Proc. IEEE* pp 673–6
[16] Tang P T 2001 *Electrochim. Acta* **47** 61
[17] Kanigicherla V K P, Kelly K W, Ma E, Wang W and Murphy M C 1998 *Microsyst. Technol.* **4** 77
[18] Zeng K and Shen L 2002 *Phil. Mag.* A **82** 2223
[19] Fritz T, Mokwa W and Schnakenberg U 2001 *Electrochim. Acta* **47** 55
[20] Zeng K and Chiu Ch 2001 *Acta Mater.* **49** 3539
[21] Ross R B 1992 *Metallic Materials Specification Handbook* 4th edn (London: Chapman and Hall)
[22] Lowenheim F 1978 *Electroplating* (New York: McGraw-Hill)
[23] van Kan J A, Bettiol A A and Watt F 2001 *Nucl. Instrum. Methods* A **181** 258
[24] Roos N, Glinsner T and Scheer H-C 2003 *Proc. SPIE* **5037** 211